

# Tidal Streams as Probes of the Galactic Potential

Kathryn V. Johnston<sup>1</sup>, HongSheng Zhao<sup>2</sup>, David N. Spergel<sup>3</sup> and Lars Hernquist<sup>4</sup>

## ABSTRACT

We explore the use of tidal streams from Galactic satellites to recover the potential of the Milky Way. Our study is motivated both by the discovery of the first lengthy *stellar* stream in the halo (Irwin & Totten 1998) and by the prospect of measuring proper motions of stars brighter than 20th magnitude in such a stream with an accuracy of  $\sim 4\mu\text{as}/\text{yr}$ , as will be possible with the Space Interferometry Mission (SIM). We assume that the heliocentric radial velocities of these stars can be determined from supporting ground-based spectroscopic surveys, and that the mass and phase-space coordinates of the Galactic satellite with which they are associated will also be known to SIM accuracy. Using results from numerical simulations as trial data sets, we find that, if we assume the correct form for the Galactic potential, we can predict the distances to the stars as a consequence of the narrow distribution of energy expected along the streams. We develop an algorithm to evaluate the accuracy of any adopted potential by requiring that the satellite and stars recombine within a Galactic lifetime when their current phase-space coordinates are integrated backwards. When applied to a four-dimensional grid of triaxial logarithmic potentials, with varying circular velocities, axis ratios and orientation of the major-axis in the disk plane, the algorithm can recover the parameters used for the Milky Way in a simulated data set to within a few percent using only 100 stars in a tidal stream.

*Subject headings:* Galaxy: fundamental parameters, halo, kinematics and dynamics, structure

---

<sup>1</sup>Institute for Advanced Study, Princeton, NJ 08450

<sup>2</sup>Sterrewacht Leiden, Niels Bohrweg 2, 2333 CA, Leiden, The Netherlands

<sup>3</sup>Princeton University Observatory, Princeton University, Princeton, NJ 08544

<sup>4</sup>Department of Astronomy and Astrophysics, University of California, Santa Cruz, CA 95064.

## 1. Introduction

Tidal streams in the Galactic halo are a natural by-product of hierarchical structure formation, in which galaxies build up their mass by accreting less massive satellites. These features can be produced when matter, *i.e.* stars and/or gas, is liberated from a companion either by tidal shocking at the pericenter of the satellite’s orbit or, in the case of globular clusters, through the evaporation of stars across the tidal boundary imposed by the Milky Way. The stripped material populates leading and trailing tidal streams that align with the orbit of the satellite for timescales comparable to or greater than the age of the Galaxy (e.g. Oh, Lin & Aarseth 1995; Grillmair et al. 1995; Johnston, Spergel & Hernquist 1995; Johnston, Hernquist & Bolte 1996, hereafter JHB).

The notion of using tidal streams as Galactic potentiometers has been considered previously by a number of authors (Lynden-Bell 1982; Kuhn 1993; Grillmair 1998; Zhao 1998). By assuming that several of the dwarf spheroidal satellites are tidal debris, Lynden-Bell (1982) was able to obtain an estimate of the mass of the Milky Way. Similarly, if the Magellanic Stream consists of gas tidally stripped from the Large and Small Magellanic Clouds, it can be used to constrain the potential (Murai & Fujimoto 1980; Lin & Lynden-Bell 1982; Lin, Jones & Klemola 1995). While these results are not definitive measurements owing to the controversial nature of the Magellanic Stream (Moore & Davis 1994), they demonstrate the power of this approach.

There is now growing observational evidence for the existence of *stellar* tidal streams in the halo. Several globular clusters are known to possess excess unbound stars outside their tidal radii (Grillmair et al. 1995; Irwin & Hatzidimitriou 1995; Kuhn, Smith & Hawley 1996) and there are also moving groups in the halo with no obvious bound counterparts (for a review see Majewski, Hawley & Munn 1996). On larger scales, the debris associated with the dwarf galaxy recently discovered in the constellation Sagittarius (Ibata, Gilmore & Irwin 1994), has now been identified in horizontal branch (HB) and giant branch (GB) stars over  $22^\circ$  along a Galactic great circle roughly coinciding with the  $l = 0^\circ$  plane (Mateo et al. 1996; Alard 1996; Fahlman et al. 1996; Ibata et al. 1997). Moreover, Irwin & Totten’s (1998) discovery of a carbon star trail encircling the Galaxy and aligned with the same plane provides the first example of a data set that samples the entire length of a stellar tidal stream.

Upcoming satellite missions promise to provide accurate phase-space coordinates for individual stars in tidal streams. NASA’s Space Interferometric Mission (SIM), scheduled for 2006, is a pointed instrument that will detect

stars as faint as 20th magnitude with accuracies of a few  $\mu\text{as}$ . ESA’s Global Astrometric Interferometer for Astrophysics (GAIA) will survey more than a billion stars across the entire sky with an astrometric precision of  $\leq 10\mu\text{as}$ . This represents an improvement over results obtained with the HIPPARCOS satellite by a factor of about a thousand in accuracy and more than a million in the volume sampled, and makes the idea of measuring the proper motions of individual HB and GB stars (and hence carbon stars) at distances  $\leq 100$  kpc feasible. At distances of tens of kiloparsecs, these future missions, when supplemented with radial velocities, will accurately measure five out of the six phase-space coordinates of a star.

In this *Letter*, we investigate the extent to which the potential of the Galaxy can be recovered using a data set such as Irwin & Totten’s (1998) carbon star stream, assuming that phase-space positions can be inferred with the accuracy of the SIM satellite. At the appropriate distances, parallaxes measured by SIM ( $\sim 4\mu\text{as}$ ) will be the least well-determined phase-space component. The implied uncertainty in distances,  $\sim (D/20\text{kpc})^2$  kpc for stars at a distance  $D$ , will exceed the thickness of the tidal stream. In §3.1, we show that using energy conservation in the correct background potential, together with the other five phase-space coordinates, yields a more precise distance estimate. We describe simulations that provide trial data sets for our proposed methods in §2, and use them to estimate the accuracy of distances to debris stars constrained by energy conservation in §3.1. We apply our algorithm for recovering the potential of the Milky Way in §3.2, and summarize conclusions in §4.

## 2. Trial Data Sets and Galactic Model

This paper is based on an analysis of simulated debris trails produced by tidal disruption, as reported in JHB. In these simulations, the Milky Way potential  $\Phi_{\text{MW}}$  was taken to be smooth, static and axisymmetric, and was represented by a three-component bulge-disk-halo model. In each simulation, the satellite was represented by  $10^4$  particles, whose self-gravity was calculated using a self-consistent field code (Hernquist & Ostriker 1992). The particles were initially distributed as a Plummer model, and evolved in the Milky Way potential for 10 Gyrs. The reader is referred to JHB for full details of the simulations.

We tested our algorithm on all the models (1-12) in JHB and, in the figures which follow, we illustrate the results using their Model 11. This satellite had an initial mass  $2.893 \times 10^7 M_{\odot}$  and scale-length 0.602kpc. It was on an orbit

inclined at  $50^\circ$  relative to the Galactic disk with an orbital period  $\sim 2$  Gyrs and peri- and apo-center distances of  $\sim 40$  kpc and  $\sim 160$  kpc. We also performed two new simulations with the same initial conditions as in Model 11, but with the spherical halo component of the Milky Way potential replaced by oblate and triaxial components of the form

$$\Phi_{\text{halo}}(x, y, z) = \frac{v_{\text{circ}}^2}{2} \ln(x^2 + y^2/p^2 + z^2/q^2 + c^2). \quad (1)$$

In the remainder of the paper we shall refer to these new simulations as Models 13 and 14. In all cases  $v_{\text{circ}} = 181$  km/s and  $c = 12$  kpc. In Models 1-12  $(p, q) = (1, 1)$ , in Model 13  $(p, q) = (1, 0.75)$  and in Model 14  $(p, q) = (0.95, 0.75)$ .

### 3. Results

#### 3.1. Energy Distances

Tidal debris tends to become unbound from a satellite of mass  $m_{\text{sat}}$  located at distance  $R$  from the center of the Galaxy on the physical scale given by the tidal radius

$$r_{\text{tide}} = R \left( \frac{m_{\text{sat}}}{M_R} \right)^{\frac{1}{3}} \quad (2)$$

(King 1962), where  $M_R$  is the mass of the Galaxy enclosed within  $R$ . Hence the orbital energies  $E$  of material in the debris will lie approximately within

$$\epsilon = r_{\text{tide}} \frac{d\Phi}{dR} = r_{\text{tide}} \frac{GM_R}{R^2} \quad (3)$$

of the satellite’s orbital energy,  $E_{\text{sat}}$  (Tremaine 1993, Johnston 1998). Equations (2) and (3) should be evaluated not at the current position of the satellite, but at the pericenter of its orbit since most of the mass loss will occur where the tidal field of the Milky Way is strongest. The top panel of Figure 1 shows  $E$  for all particles which were no longer bound to the satellite at the end of the simulation of Model 11, with the left hand axis in physical units and the right hand axis in units relative to  $E_{\text{sat}}$  and scaled by  $\epsilon$  given in equation (3). Note that the debris divides into two populations, corresponding to stars in the leading/trailing stream having  $E$  offset by  $\mp 5\epsilon/4$  from  $E_{\text{sat}}$ . Each population has a width  $\sim 3\epsilon/4$  about these average offsets.

Even with the astrometric accuracy of SIM, we will be able to measure distances only to a precision  $\gtrsim 10\%$  beyond 20 kpc. However, if we can identify a population of stars which were once associated with a satellite and we assume

a form  $\Phi_{\text{MW}}$  for the Galactic potential, it is possible to estimate their distances from the expected energy distribution in the satellite’s debris. To test this idea we “observe” the angular position  $(l, b)$ , line of sight velocity  $v_{\text{los}}$  and proper motion  $(\mu_l, \mu_b)$  of each of the unbound particles at the end of our simulations from an assumed heliocentric viewpoint in the disk plane 8.5 kpc from the center of the Galaxy, where the motions are defined in a Galactic rest frame. Each particle is assigned  $E = E_{\text{sat}} \mp 5\epsilon/4$  if it is ahead/behind the satellite along the orbit, and its heliocentric distance  $d$  is then calculated by solving the equation

$$E = \frac{1}{2} \left[ v_{\text{los}}^2 + d^2(\mu_l^2 + \mu_b^2) \right] + \Phi_{\text{MW}}(d, l, b). \quad (4)$$

The bottom panel of Figure 1 plots the error in the distance estimated for particles in Model 11 using this method. As can be seen from the right hand axis of this figure, we expect this distance estimate to be good to within a few  $r_{\text{tide}}$ . In contrast, the solid lines show the much lower accuracy of distances measured from parallaxes with the SIM satellite (as described in §1).

### 3.2. Constraining the Galactic Potential

If we observe a set of stars that were once associated with a satellite of known mass and phase-space coordinates, then they must be on orbits whose trajectories intersect with the satellite within the lifetime of the Galaxy. The following algorithm assigns a quality factor for each assumed form  $\Phi(x, y, z)$  for the Galactic potential based on how well it can extrapolate the orbits of tidal debris stars back into the progenitor satellite galaxy.

1. For each assumed potential we integrate the satellite’s orbit backwards and calculate  $r_{\text{tide}}$  (eqn [2]) and the energy scale  $\epsilon$  (eqn [3]) at pericenter.
2. For each star in the debris with measured proper motion, angular position and radial velocity we: (i) create  $n_{\text{test}}$  particles with energies  $E$  evenly distributed in the range  $\pm 3\epsilon/4$  about  $(E_{\text{sat}} \mp 5\epsilon/4)$  if the star is ahead/behind the satellite along its orbit; (ii) estimate the “energy-distance” to each particle; (iii) integrate both the satellite and these particles backwards in time in the assumed potential for a Galactic lifetime; and (iv) credit the potential with a capture whenever any one of these particles is separated from the satellite by a distance  $dr < 1.8 r_{\text{tide}}$  and a velocity  $dv < \sqrt{\frac{Gm_{\text{sat}}}{dr}}$ .
3. Assign the potential’s “score” as the number of successful captures, with the most likely potential having the highest score.

We tested this algorithm by applying it to 128 stars selected at random at the end of each simulation. For each star, 10 test particles were integrated in a four-dimensional grid of halo potentials of the form given in equation (1) with  $v_{\text{circ}}, q$  and  $p$  varied by 10% around the values in the simulations, and  $x$  and  $y$  axes rotated between 0-90 degrees. The left hand panels of Figure 2 show the maximum number of recaptured particles after 10 Gyrs at fixed  $v_{\text{circ}}$  but varying  $p, q$  and orientation of the  $x$  and  $y$  axes, for Models 11 (top), 13 (middle) and 14 (bottom). The right hand panels show contours of the maximum number of recaptured particles in the  $p - q$  plane for arbitrary axis orientation and  $v_{\text{circ}}$  corresponding to the maximum in the left hand panels. The points corresponding to the parameters of the potential in which the simulations were originally run are marked with solid squares and the recovered parameters are marked with stars. The figure demonstrates that this method is sensitive to both the mass distribution and the geometry of the Milky Way.

We can estimate the error introduced by using  $N$  stars to determine the potential from the bootstrap method. We create  $N(\log N)^2$  data sets, each of size  $N$ , by drawing stars at random (with replacement) from the original sample. For each set, we estimate the Milky Way parameters corresponding to the grid cell with the maximum score as outlined above. It has been shown (see Babu & Feigelson 1996 and references therein), that the distribution of these bootstrapped estimates around the original one will closely follow the intrinsic distribution of errors due to sampling. Figure 3 shows the dispersion  $\sigma_w$  (defined as  $\sigma_w = \sqrt{\langle w^2 \rangle - \langle w \rangle^2}$ , where the angles denote averaging) of our bootstrapped distribution of estimates for  $v_{\text{circ}}, q$  and  $p$  as a function of  $N$ . The line in bold corresponds to  $\sigma_w \propto 1/10\sqrt{N}$ . The figure shows that the circular velocity and axis ratios of the Milky Way can be recovered to within a few percent using just 100 stars associated with one of the dwarf spheroidal satellites.

#### 4. Conclusion: You Can Judge a Galaxy by Its Tail

In this *Letter*, we have explored the use of SIM measurements of stars in tidal streams as a probe of the Galactic potential. We find that with five-dimensional phase-space information for only 100 stars, we can determine the circular velocity and shape of the Galactic halo with accuracies of a few percent. This measurement would represent more than an order-of-magnitude improvement in our knowledge about the Galaxy’s mass distribution (Kochanek 1996; Zhao 1998).

It should be noted, however, that our discussion has been limited to

constraining four parameters in a specific assumed form for the Galactic potential. Ultimately, as with any parameterized inversion algorithm, the uncertainty of the method will increase with the number of parameters varied. One issue which we have not considered is the degree to which the method discussed here can be used to constrain the total extent of the Galactic halo, in a manner analogous to that which has been applied recently to tidal tails in merging galaxies (*e.g.* Dubinski et al. 1996, 1998; Springel & White 1998). Naively, we expect the measurements proposed here to be most sensitive to the mass of the Galaxy enclosed within the region occupied by the debris comprising a stream. However, the unusually high precision offered by SIM suggests that the influence of the mass distribution on larger scales could be probed if the halo is highly flattened.

The spatial distribution of matter in the Galaxy provides insight into both the formation history of our Galaxy and the nature of dark matter. In future work we will look at the evolution of tidal debris in lumpy or time-dependent potentials and discuss using tidal streams to measure not only the current state of the Milky Way, but also to infer its history.

We thank Mike Irwin and Ed Totten for telling us about the results of their carbon star survey and Tim de Zeeuw and John Bahcall for helpful comments on the paper. KVJ acknowledges the support of funds from the Institute for Advanced Study and thanks the Institute of Astronomy (Cambridge) for the visitors grant used while putting the final touches on the paper. HSZ would like to acknowledge a travel grant from the Leids Kerkhoven-Bosscha Fonds and to thank Princeton Observatory for hospitality during the visit that resulted in this collaboration. DNS's work on this project was partially supported by NASA ATP grant NAG 5-7066, and LH was supported in part by NASA theory grant NAG5-3059 and by the NSF under grants ASC 93-18185 and ACI-96-19019.

## REFERENCES

- Alard, C. 1996, ApJ, 458, L17
- Babu, G.J. & Feigelson, E.D. 1996, “Astrostatistics”, (Chapman & Hall, London)
- Dubinski, J., Mihos, J.C. & Hernquist, L. 1996, ApJ, 462, 576
- Dubinski, J., Hernquist, L. & Mihos, J.C. 1998, in Galactic Halos: A UC Santa Cruz Workshop, ASP Conf. Ser. Vol 136, ed. D. Zaritsky, (ASP, San Francisco), p. 260
- Fahlman, G. G., Mandushev, G., Richer, H. B., Thompson, I. B. & Sivaramakrishnan, A. 1996, ApJ, 459, L65
- Grillmair, C.J., 1998, astro-ph/9711223
- Grillmair, C.J., Freeman, K.C., Irwin, M. & Quinn, P.J. 1995, AJ, 109, 2553
- Hernquist, L. & Ostriker, J.P. 1992, ApJ, 386, 375
- Ibata, R. A., Gilmore, G. & Irwin, M. J. 1994, Nature, 370, 194
- Ibata, R. A., Wyse, R.F.G., Gilmore, G., Irwin, M. J. & Suntzeff, N.B. 1997, AJ, 113, 634
- Irwin, M. J. & Hatzidimitriou, D. 1995, MNRAS, 277, 1354
- Irwin & Totten 1998, in preparation
- Johnston, K.V. 1998, ApJ, 495, 297
- Johnston, K. V., Hernquist, L. & Bolte, M. 1996, ApJ, 465, 278 (JHB)
- Johnston, K. V., Spergel, D. N. & Hernquist, L. 1995, ApJ, 451, 598
- King, I. R. 1962, AJ, 67, 471
- Kochanek, C. 1996, ApJ, 457, 228
- Kuhn, J. R. 1993, ApJ, 409, L13
- Kuhn, J. R., Smith, H. A. & Hawley, S. L. 1996, ApJ, 469, L93
- Lin, D.N.C. & Lynden-Bell, D. 1982, MNRAS, 198, 707
- Lin, D.N.C., Jones, B.F. & Klemola, A.R. 1995, ApJ, 439, 652
- Lynden-Bell, D. 1982, Observatory, 102, 202
- Majewski, S. R., Hawley, S. L. & Munn, J. A. 1996, in The Formation of the Galactic Halo: Inside and Out, ASP Conf. Ser. Vol 92, eds. H. Morrison & A. Sarajedini, (ASP, San Francisco), p. 119



- Mateo, M., Mirabel, N., Udalski, A., Szymański, M., Kubiak, M., Krzemiński, W. & Stanek, K. Z. 1996, *ApJ*, 458, L13
- Miyamoto, M. & Nagai, R. 1975, *PASJ*, 27, 533
- Moore, B. & Davis, M. 1994, *MNRAS*, 270, 209
- Murai, T. & Fujimoto, M. 1980, *PASJ*, 32, 581
- Oh, K.S., Lin, D.N.C. & Aarseth, S.J. 1995, *ApJ*, 442, 142
- Springel, V. & White, S.D.M. 1998, *astro-ph/9807320*
- Tremaine, S. 1993 in *Back to the Galaxy* eds. S. S. Holt & F. Verter, (*AIP Conf. Proc.* : New York), p. 599
- Zhao, H.S. 1998, *ApJ*, 500, L149

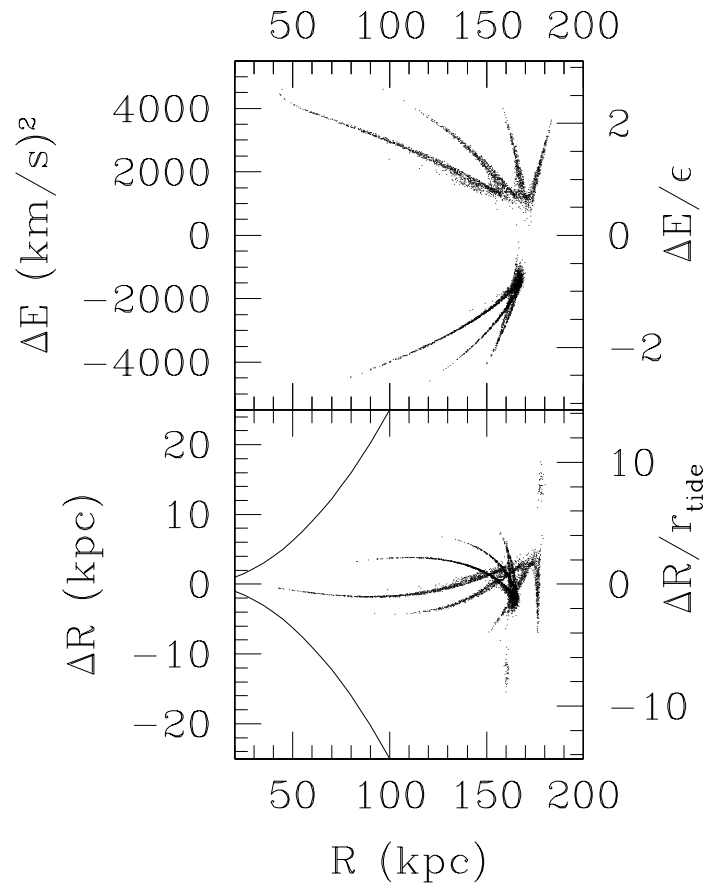


Fig. 1.— Top panel — orbital energy relative to the satellite’s  $\Delta E$  for all particles unbound at the end of the simulation of Model 11. Bottom panel — error in the distance estimate described in §3.1. The solid lines show the accuracy of distances derived from SIM parallax measurements.

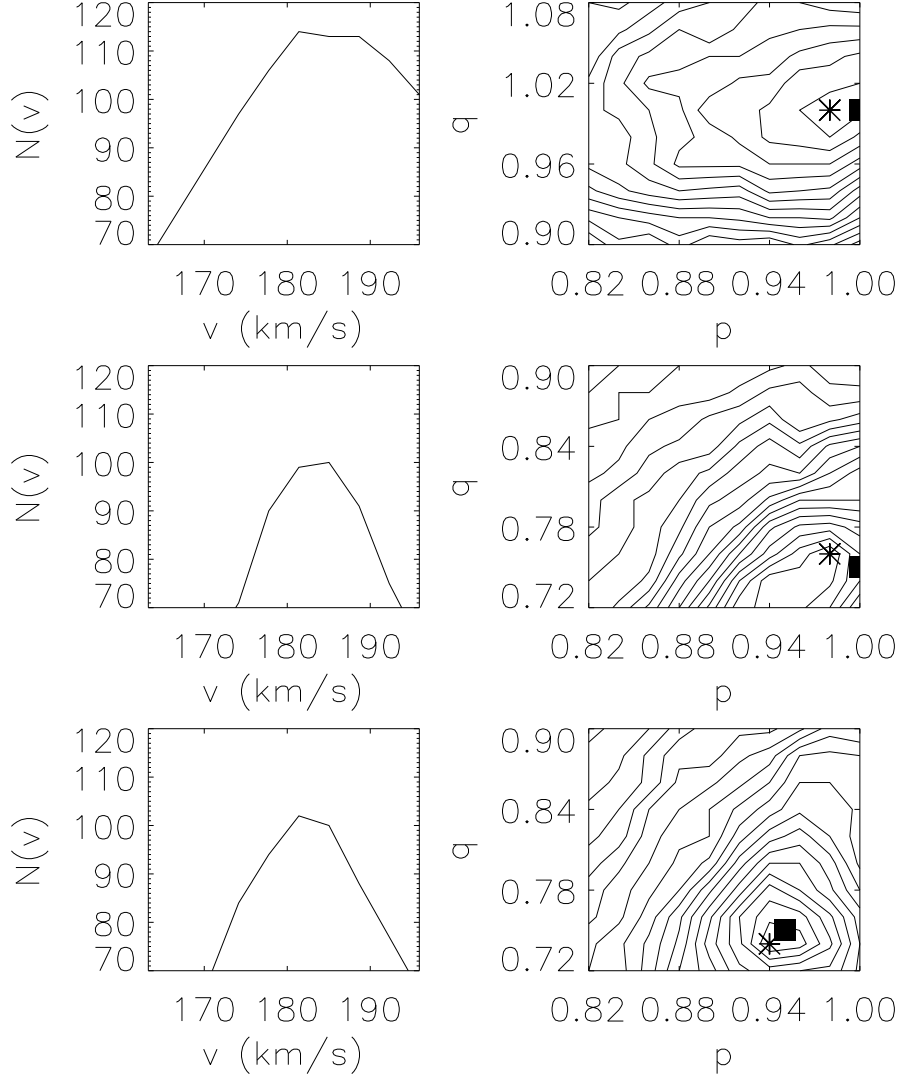


Fig. 2.— Left hand panels — maximum number of captured particles for fixed  $v_{\text{circ}}$  and arbitrary  $q, p$  and axis orientation as a result of applying our algorithm to Models 11 (top panel), 13 (middle panel) and 14 (bottom panel). Right hand panels — maximum number of rebound particles contoured in the  $p$ - $q$  plane for the most-likely value of  $v_{\text{circ}}$  identified in the left-hand panels. The maxima corresponding to the most likely parameters are marked with stars, and the parameters actually used in the simulations are shown with solid squares. The contours are spaced by 4 particles.

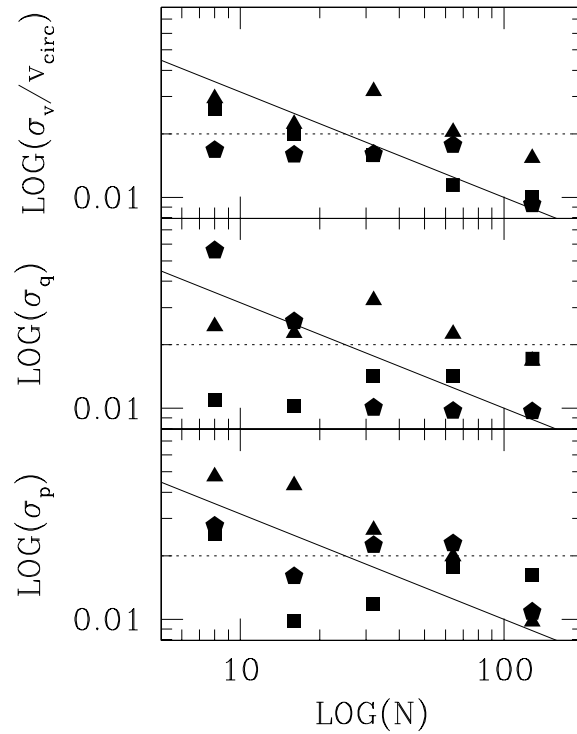


Fig. 3.— Bootstrapped errors in the potential calculated with  $N$  stars. The solid triangles, squares and pentagons are for Models 11, 13 and 14 respectively. The bold line is given by  $\sigma_w = 1/10\sqrt{N}$ . The dotted line shows the size of one cell of the gridded distribution from which  $\sigma_w$  was calculated.